

# Low-threshold electron-beam-pumped green quantum-well heterostructure semiconductor lasers

M.M. Zverev, D.V. Peregoudov, I.V. Sedova, S.V. Sorokin, S.V. Ivanov, P.S. Kop'ev

**Abstract.** The parameters of 494–555-nm Cd(Zn)Se/ZnMgSSe green lasers with differently designed active regions pumped by a 8–30-keV electron beam are studied. The minimum threshold current density (0.6–0.8 A cm<sup>-2</sup> at room temperature) is obtained for a structure with the active region consisting of a ZnSe quantum well with a CdSe fractional monolayer insertion.

**Keywords:** electron-beam-pumped laser, quantum-well structure.

Although electron-beam-pumped semiconductor lasers [1] have been known for more than three decades, they have not still been in wide use. This is explained mainly by the high threshold pump-power density, the high voltage, and cryogenic cooling, which is often used to provide the operation of such lasers. The limiting values of the pulse and mean power in electron-beam-pumped semiconductor lasers were obtained for the structures in which single crystals were used as active media. A considerable decrease in the threshold current density and the operating energy of the electron beam can be expected when using heterostructures similar to those widespread in injection lasers. Zinc-selenide-based structures are most suitable for the blue–green spectral region. The possibilities of using them in electron-beam-pumped lasers were studied insufficiently.

The use of epitaxial ZnSe films on ZnS substrates for electron-beam-pumped lasers was first reported in [2, 3]. The transverse pumping by a 50-keV electron beam [3] resulted in lasing with a threshold current density of 4.5 A × cm<sup>-2</sup> ( $T \sim 80$  K) and 42 A cm<sup>-2</sup> ( $T = 300$  K). In cooled (80 K) and transversely pumped lasers on ZnSe films grown on GaAs substrates using the method of metalorganic chemical vapour deposition, a threshold current density of 3.5 A cm<sup>-2</sup> was achieved upon pumping by 30–45-keV

electrons [4]. Lasing was attained on ZnSe films and a ZnSe/ZnSSe superlattice grown by the molecular beam epitaxy (MBE) method [5]. The threshold current density obtained in these lasers at room temperature was 5 and 12 A cm<sup>-2</sup>, respectively (35-keV transverse pumping). By using multi-layer ZnCdSe/ZnSe quantum-well (QW) heterostructures in lasers longitudinally pumped by a scanning electron beam, an average output power of a few watts was achieved in a quasi-cw mode at room temperature [6, 7]. The lasing threshold was  $> 1$  MW cm<sup>-2</sup> at an electron-beam energy of 30–70 keV. The use of miniature field-emission electron sources to pump QW lasers made it possible to achieve lasing at beam energies of  $\sim 10$  keV in the IR region at room temperature [8] and in the blue–green region for samples cooled to cryogenic temperatures [9].

Due to deep cryogenic cooling (down to 20 K), an extremely low threshold pump-energy density of 450 W × cm<sup>-2</sup> was achieved for a laser based on a ZnCdSe QW and pumped by a 5-keV electron beam [10, 11]. QW heterostructures based on ZnSe with a short-period superlattice (SL) were used as waveguides and allowed us to obtain lasing in blue–green lasers at a threshold current density of  $\sim 3$ –3.5 A cm<sup>-2</sup>, electron-beam energies of 15–30 keV, and room temperature [12, 13].

This paper presents the results of studying lasing properties of electron-beam-pumped Cd(Zn)Se/ZnMgSSe heterostructures with various types of the active region.

(Zn, Mg)(S, Se) structures for electron-pumped lasers were grown pseudomorphously on GaAs (001) substrates at  $T = 270$ –280 °C by the MBE method. These structures contain lower and upper  $Zn_{0.9}Mg_{0.1}S_{0.15}Se_{0.85}$  cladding layers with thicknesses  $h = 0.7$  and 0.1–0.2 μm, respectively, a symmetric waveguide in the form of a lattice with layers 15 Å-ZnS<sub>0.14</sub>Se<sub>0.86</sub>/18 Å-ZnSe with a total thickness of 0.2 μm, and the active region in the form of an ordinary isolated ZnCdSe QW (a first-type structure) or a ZnSe QW with a depth of 10 nm (a second-type structure) containing a CdSe fractional monolayer insertion at its centre (Fig. 1). When being deposited on the ZnSe surface, the CdSe layer with a nominal thickness of 2.5 monolayers is transformed into an array of self-organising CdSe-enriched nanoislands (quantum disks). This is caused by an elastic relaxation of stresses due to the lattice parameter mismatch ( $\Delta a/a \sim 7\%$ ). Lasing with the extremely low threshold pump power density ( $\sim 4$  kW cm<sup>-2</sup>) was attained earlier in optically pumped lasers based on such structures [14]. Specific features of growing the active region on the basis of CdSe quantum disks by the MBE method are described in detail in [15].

**M.M. Zverev** State Research Center of the Russian Federation, Troitsk Institute for Innovation and Fusion Research, 142092 Troitsk, Moscow region, Russia; e-mail: mzverev@triniti.ru;

**I.V. Sedova, S.V. Sorokin, S.V. Ivanov, P.S. Kop'ev** A.F. Ioffe Physicotechnical Institute, Russian Academy of Sciences, 194021 St. Petersburg, Russia;

**D.V. Peregoudov** Moscow State Institute of Radio Engineering, Electronics, and Automation (Technical University), pr. Vernadskogo 78, 117454 Moscow, Russia

Received 28 June 2004

*Kvantovaya Elektronika* 34 (10) 909–911 (2004)

Translated by A.S. Seferov

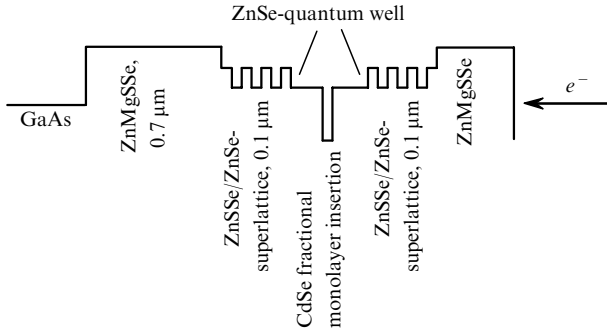


**Figure 1.** Scheme of a semiconductor structure and a ZnSe quantum well with a CdSe fractional monolayer insertion.

The use of an alternately stressed short-period superlattice makes it possible to increase the electron confinement for holes at an optimal optical confinement, to improve the efficiency of carrier collection and the resistance of the entire structure to mechanical stresses, and to protect the active region against penetration and development of extended and point defects [16].

All measurements were performed at room temperature under transverse excitation without depositing a reflecting coating on the crystal faces. The diameter of the pump pulsed electron beam could be varied in the sample plane. Its minimum size was 0.3 mm. The electron energy could be varied from 8 to 30 keV, and the pump pulse duration was  $\sim 50$  ns at a pulse repetition rate of  $< 10$  Hz. The lasing spectra were recorded with a linear CCD array, which was fixed at the exit of an MDR-2 monochromator. A calibrated coaxial FEK-22 photocell was used to measure the light-pulse profile and the lasing power. The lasing threshold was determined visually as the appearance of a bright luminescent point at the sample end accompanied by a sharply narrowed radiation pattern.

The threshold current density as a function of the electron-beam energy at different resonator lengths was measured for various structures.

When the electron-beam energy changes from 30 to 8 keV, the threshold current density initially falls and reaches a minimum at energies of 15–20 keV and then begins to increase with a further decrease in the beam energy (Fig. 2). The minimum threshold current density ( $0.6\text{--}0.8 \text{ A cm}^{-2}$ ) was obtained for the second-type structure ( $L = 1.35$  mm) at a beam energy of 15–18 keV and a threshold power density of  $\sim 10 \text{ kW cm}^{-2}$ .

The maximum pulsed output power was 9 W. As the pump power increased after the maximum output power had been achieved, a decrease in the latter was observed, which was evidently caused by a damage in the semiconductor structure. For an output power of  $\sim 0.5$  W ( $U = 20$  kV) and a pulse repetition rate of 10 Hz, the former remained unchanged for 30 min. In our experimental setup, the maximum current from the electron gun falls with a decrease in the accelerating voltage, and the output lasing power also depends on the electron-beam energy. For an accelerating voltage  $U = 8$  kV, the maximum output pulse power was 0.2 W.

The maximum lasing efficiency defined as the ratio of the output power emerging through one face to the power of the pump electron beam was  $< 1.6\%$  for all structures and was reached at electron-beam energies of 17–21 keV. Note that

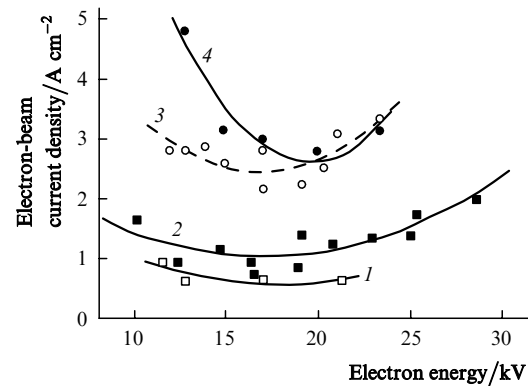


**Figure 2.** Threshold current density as a function of the electron-beam energy for second-type (1, 2, 4) and first-type (3) semiconductor structures at  $h = 0.1$  (1, 2, 3) and  $0.2 \mu\text{m}$  (4) and  $2L = 1.35$  (1), 0.95 (2), 0.5 (3), and 0.62 mm (4).

a considerable fraction of the electron beam was lost in the substrate, since the electron-beam penetration depth into the ZnSe crystal at such energies is  $\sim 1\text{--}1.5 \mu\text{m}$  [17], which far exceeds the distance from the active region to the sample surface ( $0.2 \mu\text{m}$ ) in the structures studied by us. In order to utilise the pump energy more efficiently, the structure must be fitted more precisely to the electron-beam energy. As the latter decreases resulting in a decrease in the depth of the excited region, the role of the pump-energy losses in the structure's outer layers that face its surface becomes more significant. When the thickness  $h$  of the upper cladding decreases from 0.2 to 0.1  $\mu\text{m}$ , the electron-beam energy at which the minimum threshold current density is observed falls from 18–20 to 15–16 keV. Thus, using thicker structures with thinner surface layers can increase the lasing efficiency.

The lasing wavelength for different structures lies between 494 and 555 nm, and the linewidth is 2–3 nm (Fig. 3). For each structure, the wavelength at the peak of the emission line varies depending on the electron-beam energy and the resonator length.

The laser radiation pattern is highly asymmetric. The divergence is  $> 30^\circ$  in the plane passing through the axes of the electron beam and laser resonator. In the plane of the semiconductor structure, the far-field distribution was quite

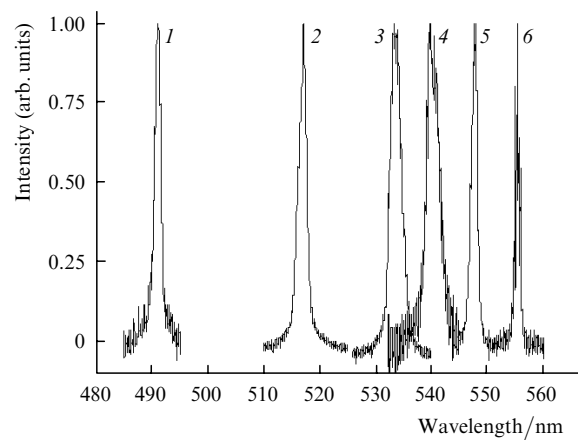


**Figure 3.** Generation spectra of lasers on first-type (1, 2, 6) and second-type (3, 4, 5) semiconductor structures.

complex and consisted of a large number of narrow peaks. The mean half-width of the radiation pattern for most of samples was  $2^\circ - 5^\circ$  (depending on the pump and resonator parameters).

Hence, the use of ZnSe-based QW heterostructures with a SL waveguide, which are pumped by an electron-beam energy of 8–30 keV, allows lasing to be realised in the blue-green region at room temperature. The minimum threshold beam-current density ( $0.6 - 0.8 \text{ A cm}^{-2}$ ) was observed for a structure with a CdSe fractional monolayer insertion. The low threshold electron-beam-current densities obtained experimentally at moderate accelerating voltages and room temperature make it possible to create compact sealed-off devices – electron-beam-pumped lasers.

**Acknowledgements.** This work was supported by the Federal Program ‘Research of High School in Priority Trends of Science and Technology’ (Project No. 208.05.01.044), Ministry of Education (Grant No. E02-3.1-209), and INTAS (Grant No. 03-51-5019). S.V. Ivanov is also grateful to the Russian Science Support Foundation.

## References

- doi> 1. Bogdankevich O.V. *Kvantovaya Elektron.*, **21**, 1113 (1994) [*Quantum Electron.*, **24**, 1031 (1994)].
2. Bogdankevich O.V., Lavrushin B.M., Matveev O.V., Pevtsov V.F., Khalimon M.M. *Kvantovaya Elektron.*, **3**, 612 (1976) [*Sov. J. Quantum Electron.*, **6**, 329 (1976)].
3. Petukhov V.S., Pechenov A.N., Talenskii O.N., Khalimov M.M. *Kvantovaya Elektron.*, **5**, 682 (1978) [*Sov. J. Quantum Electron.*, **8**, 400 (1978)].
4. Bogdankevich O.V., Zhuravlev L.A., Konovalov A.D., et al. *Kvantovaya Elektron.*, **10**, 1007 (1983) [*Sov. J. Quantum Electron.*, **13**, 632 (1983)].
- doi> 5. Cammack D.A., Dalby R.J., Cornelissen J.J., Khurgin J. *J. Appl. Phys.*, **62**, 3071 (1987).
6. Basov N.G., Dianov E.M., Kozlovskii V.I., Krysa A.B., Nasibov A.S., Popov Yu.M., Prokhorov A.M., Trubenko P.A., Shcherbakov E.A. *Laser Phys.*, **6** (3), 608 (1996).
- doi> 7. Basov N.G., Dianov E.M., Kozlovskii V.I., Krysa A.B., Nasibov A.S., Popov Yu.M., Prokhorov A.M., Trubenko P.A., Shcherbakov E.A. *Kvantovaya Elektron.*, **22**, 756 (1995) [*Quantum Electron.*, **25**, 726 (1995)].
- doi> 8. Molva E., Accomo R., Labrunie G., Cibert J., Bodin C., Dang L.S., Fenillet G. *Appl. Phys. Lett.*, **62**, 796 (1993).
- doi> 9. Herve D., Accomo R., Molva E., Vanzetti L., Paggel J.J., Sorba L., Francioci A. *Appl. Phys. Lett.*, **67**, 2144 (1995).
- doi> 10. Potts J.E., Smith T.L., Cheng H. *Appl. Phys. Lett.*, **50** (1), 7 (1987).
- doi> 11. Trager-Cowan C., Bagnall D.M., McGow F., McCallum W., O'Donnell K.P., Smith P.C., Wright P.J., Cockayne B., Prior K.A., Mullins J.T., Horsburgh G., Cavenett B.C. *J. Cryst. Growth*, **159**, 618 (1996).
12. Zverev M.M., Sorokin S.V., Sedova I.V., Peregovodov D.V., Ivanov S.V., Kop'ev P.S. *Phys. Stat. Sol. (b)*, **229** (2), 1025 (2002).
13. Zverev M.M., Ivanov S.V., Peregovodov D.V., Sorokin S.V., Sedova I.V., Kop'ev P.S. *Poverkhnost. Rentgen. Sinkhrotron. Neutron. Issled.*, **9**, 22 (2002).
- doi> 14. Ivanov S.V., Toropov A.A., Sorokin S.V., Shubina T.V., Lebedev A.V., Sitnikova A.V., Kop'ev P.S., Alferov Z.I. *J. Cryst. Growth*, **201/202**, 942 (1999).
- doi> 15. Ivanov S.V., Toropov A.A., Shubina T.V., Sorokin S.V., Lebedev A.V., Kop'ev P.S., Posina G.R., Bergman J.P., Monemar B. *J. Appl. Phys.*, **83**, 3168 (1998).
- doi> 16. Ivanov S.V., Toropov A.A., Sorokin S.V., Shubina T.V., Lebedev A.V., Kop'ev P.S., Alferov Zh.I., Lugauer H.-J. Reuscher G., Keim M., Fischer F., Waag A., Landwehr G. *Appl. Phys. Lett.*, **73**, 2104 (1998).
17. Trager-Cowan C., Yang F., O'Donnell K.P. *Adv. Mater. Optics and Electronics*, **3**, 295 (1994).